

Research Article

Ferromagnetic Biochar Derived from Agricultural Waste of *Musa acuminata* for Adsorption of Dyes

Alexander Gaitán Bermúdez*, Maria Jose Arbeláez Arias, Julio Cesar Mosquera and Deibys Josue Marquez Castro Optoelectronics group, Interdisciplinary Institute of Sciences, University of Quindío, Armenia, Quindío, Colombia

* Corresponding author. E-mail: agaitanb@uniquindio.edu.co DOI: 10.14416/j.asep.2025.06.004

Received: 16 December 2024; Revised: 11 April 2025; Accepted: 28 April 2025; Published online: 5 June 2025

© 2025 King Mongkut's University of Technology North Bangkok. All Rights Reserved.

Abstract

Dyes used in different industries are one of the main sources of water pollution. In this study, ferromagnetic biochar derived from agricultural residues of *Musa acuminata* was investigated as an adsorbent of dyes from water contaminated with methylene blue and rhodamine b. Biochar was obtained by pyrolysis at 550 °C for 1 h and then subjected to surface modification with FeSO₄. Morphology and surface structure were observed by scanning electron microscopy (SEM) with energy-dispersive X-ray spectroscopy (EDS). Functional groups before and after surface modification were determined using Fourier transform infrared (FTIR) spectra and Raman microscopy. Adsorption experiments were conducted in aqueous solutions previously contaminated with dyes. FTIR and Raman analyses were performed after sorption of the dyes. Adsorption kinetic analyses were performed using pseudo-first-order and pseudo-second-order models along with Intra-particle diffusion analysis. SEM-EDS revealed the biochar porosity and evidenced the presence of Fe in the material structure. FTIR and Raman analysis displayed bands associated with the surface modification with Fe. In the adsorption experiment, a maximum removal of methylene blue of 99.44% and rhodamine b of 98.20% was obtained. FTIR and Raman showed bands associated with dye adsorption. The second-order model described the adsorption kinetics. The ferromagnetic biochar from *Musa acuminata* demonstrated effective dye adsorption and could be considered an economical and environmentally friendly solution for water decontamination.

Keywords: Contaminated water, Dyes, Ferromagnetic biochar, Kinetic, *Musa acuminata*

1 Introduction

In different parts of the world deterioration of water sources is increasing. Industrial and domestic waste contaminates water sources with heavy metals, dyes, chemicals, pharmaceuticals, insecticides or pesticides, among others [1]. Dyes used in the textile industry and tanneries, present in wastewater negatively impact ecosystems and water resources [2]. Furthermore, these dyes can cause various diseases in humans and animals [3]. Organic dyes such as rhodamine b are widely used in industries such as paper, textile, leather, food, and they are also employed as dyes in printing. Studies show that rhodamine b is resistant to natural degradation and consequently affects the health of living beings [4], [5].

Some traditional water decontamination treatments involve the use of large amounts of energy, which

could generate negative impacts on the environment, making it necessary to continue searching for sustainable alternatives for water treatments [6].

Treatments such as electrocoagulation, photocatalysis, ultrasound and absorption with activated carbon have been used in the treatment of water contaminated with dyes and have shown great effectiveness [7]. The demand for activated carbon is increasing, and the gap between demand and supply is widening. As a result, the cost of activated carbon is rising, and its widespread use is being restricted [8]. In contrast, biochar derived from plant biomass is less expensive to produce and has a low environmental impact during production. Moreover, absorbing dyes with activated carbon completely removes dye molecules without leaving fragments in the water, which is why it is widely used [9]. Therefore, adsorption is a promising technique for the removal of

dyes and heavy metals using porous materials such as activated carbon and biochar. In this sense, biochar derived from agro-industrial waste has shown to be an efficient alternative as a contaminant adsorbent.

Biochar is a carbonaceous material synthesized from organic raw materials through a process called pyrolysis; the raw material for the synthesis of biochar can come from plant biomass and agro-industrial waste [10]. This material is rich in carbon, has a high cation exchange capacity, large surface area and highly porous structure [11]. Biochar has been synthesized from different precursors such as bamboo, peels of different fruits, straw and wood [12]–[18].

Biochar applications have been utilized in a variety of environmental applications such as soil remediation, dye and heavy metal removal, and carbon sequestration. Some research has focused on the employment of bamboo-derived biochar for soil remediation contaminated with heavy metals. The results demonstrated the effectiveness of bamboo biochar in the removal of Cd, Zn, Cu, and Pb showing that it can effectively remediate multiple heavy metals present in contaminated soils [19]–[21]. Similarly, biochar obtained from peels of different fruits such as banana, potato, orange, watermelon, has been used for water pollution treatment. Fruit peel biochar is effective in removing hazardous substances and metals from water such as lead, phosphate, cadmium, and copper [22]–[25]. Additionally, biochar derived from corn straw and rice straw has been used in CO₂ adsorption. Studies have shown that straw biochar can serve as potential adsorbent for CO₂, with performance comparable to that of commercial activated carbon [26], [27]. Likewise, biochar obtained from softwood and hardwood waste has been investigated in environmental applications including CO₂ sequestration and the removal of heavy metals in soils and water, demonstrating effectiveness in reducing toxic substances and polluting metals [28]–[30].

In the central region of Colombia, agro-industry is one of the main economic sources. *Musa acuminata* is one of the products with the highest density in plantations with around 7.5 t ha⁻¹ cultivated [31]. In the *Musa acuminata* harvest, the pseudostem produces a greater amount of waste, which accumulates in the plantation without any use; these wastes could be a source of raw material for biochar synthesis [32]. Furthermore, biochar derived from *Musa acuminata* presents an environmentally friendly and cost-effective solution for treating contaminated water. In this context, agricultural residues from *Musa acuminata* gain added value by being utilized in the

synthesis of by-products such as biochar. Different investigations show the use of biochar derived from banana biomass as a dye adsorbent with promising results [33], [34]. Daffalla *et al.*, [35] investigated the adsorption of Congo red dye from wastewater using pyrolyzed banana peel biochar produced at 600 °C for 1 h. They found that the biochar exhibited a predominantly mesoporous structure and achieved up to 85% dye adsorption. Similarly, Fuentes-Gandara *et al.*, [36] studied the direct removal of navy blue dye using banana peel biochar. By applying two pyrolysis temperatures (300 °C and 500 °C), they demonstrated that the biochar obtained at 500 °C achieved remarkable removal rates of up to 97% in contaminated water.

The adsorption capacity of biochar can be enhanced through surface modifications. The introduction of magnetic elements to impart magnetic properties to biochar alters its physical and chemical characteristics, increases porosity, and improves adsorption capacity in wastewater treatment. These modifications also expand its potential applications in soil remediation and heavy metal removal [37], [38].

In this study, biochar was synthesized by basic pyrolysis from pseudostem of *Musa acuminata* agro-industrial waste and was superficially modified with FeSO₄ to obtain ferromagnetic biochar (FMB), and its adsorption on dyes in aqueous solution was studied. The physical-chemical properties of FMB were analyzed before and after absorption of methylene blue (MB) and rhodamine b (RB) dyes, using a UV-vis spectrophotometer, Fourier transform infrared spectroscopy (FTIR), Raman spectroscopy, scanning electron microscope (SEM). This research shows the use of waste material and proposes the management of this waste and sustainable use of resources through the synthesis of adsorbent biochar from *Musa acuminata*.

2 Materials and Methods

2.1 Materials

Musa acuminata pseudostem waste was collected in plantations located in the central Andes region of Colombia, specifically in the Quindío department. Laboratory-grade NaOH was purchased from Merck KGaA, (Darmstadt, Germany). For biochar surface treatment, ferrous sulfate (FeSO₄) was purchased from Adbaquim S.A.S in analytical purity. Methylene blue (MB), and rhodamine b (RB) were purchased from Sigma Aldrich.

2.2 Preparation of biochar and ferromagnetic biochar (FMB)

Musa acuminata pseudostem was placed in a drying oven at 40 °C for 24 h. After the drying time, pseudostem was placed in a knife mill until particles with an approximate size of 8 mm were obtained. Subsequently, 40 g of the precursor material was packaged in a cylindrical stainless steel tube to limit its exposure to oxygen. Then, the tube was taken to a muffle furnace to perform a basic pyrolysis process at 550 °C for 1 h. The pyrolysis temperature was selected based on Tomczyk *et al.*, [39] where it is shown that at temperatures above 500 °C lignin and other organic matter are degraded, porosity and hydrophobicity increase, and yield percentage increases. The produced biochar was left at room temperature for 2 h. Biochar samples were stored in a glass desiccator for later characterization. Biochar surface was modified to obtain ferromagnetic biochar (FMB) [40]. Ferrous sulfate (FeSO_4) was used for the magnetization of biochar. This compound is easy to manipulate, inexpensive, non-toxic to the environment and is used in water treatment for the adsorption of various pollutants [41]. For surface modification, 30 g of FeSO_4 were added to a 0.5 M NaOH solution and placed under magnetic stirring. Then, 10 g of *Musa acuminata* biochar was added, and the mixture was kept under magnetic stirring at 80 °C for 2 h. The resulting mixture was filtered and washed with distilled water, then dried in a laboratory oven at 105 °C for 24 h. Finally, FMB was stored in a glass desiccator.

2.3 Characterization of biochar and ferromagnetic biochar (FMB)

Biochar morphology and surface structure were observed by scanning electron microscopy coupled with energy dispersive X-ray spectroscopy EDS (Lyra 3-Dual Beam SEM-FIB, Tescan) before and after the surface treatment process. Functional groups available on *Musa acuminata* waste biochar before and after surface treatment by FTIR (IR Prestige-21, SHIMADZU) in wavenumber ($400\text{--}4000\text{ cm}^{-1}$) and Raman spectra using a micro-Raman spectrometer (XploRA PLUS, Horiba) provided with a 785 nm laser.

2.4 Dyes adsorption experiments

Different solutions of 25 mL were prepared with the addition of 5 ppm of the dyes (MB and RB). To each

of the previously described solutions, 200 mg of FMB was added and stirred using a magnetic stirrer at 150 rpm at room temperature. The pH of the solutions was measured during the adsorption experiment, the aqueous medium was found to be acidic with a pH of 4 and showed no significant changes. Liquid samples of each solution were taken every 15 min and analyzed immediately on a UV-vis spectrophotometer (Thermo Scientific, Evolution 201/220 UV-Visible) to determine the dye concentration. In addition, FTIR and Raman analyses were performed after dye sorption. Three replicates were used, and the average value of each adsorption experiment was analyzed.

The quantity of dye adsorbed onto the FMB (q_t) and the dye removal rate from the solution (Removal) was derived from the following Equations (1) and (2):

$$\text{Removal (\%)} = \frac{C_0 - C_e}{C_0} * 100\% \quad (1)$$

$$q_t = \frac{C_0 - C_t}{m} * V \quad (2)$$

Where C_e is equilibrium concentration (mg/L), C_0 and C_t are the initial concentration of dyes and the concentration at time t (mg L^{-1}), respectively; q_t is the adsorption amount of the adsorbent at time t (mg g^{-1}); m and V are the mass of FMB (g) and the volume of dyes solution (L), respectively.

A kinetic study was performed to determine the equilibrium time and the adsorption rate. Two kinetic models, pseudo-first-order (PFO) and pseudo-second-order (PSO) were used to calculate the rate constant in the sorption process. The reaction mechanism of PFO and PSO was calculated using Equations (3) and (4), respectively.

$$\ln(q_e - q_t) = \ln q_e - K_1 t \quad (3)$$

$$\frac{t}{q_t} = \frac{1}{K_2 q_e^2} + \frac{t}{q_e} \quad (4)$$

Where q_e and q_t are the adsorbed dye at equilibrium and time, K_1 is the pseudo-first-order adsorption rate constant (min^{-1}), and K_2 is the pseudo-second-order adsorption rate constant ($\text{g/mg}\cdot\text{min}$).

Also, the rate constant of the intraparticle diffusion model K ($\text{mg/g}\cdot\text{min}^{0.5}$) was calculated for each of the dyes using the following Equation (5):

$$q_t = Kt^{0.5} + C \quad (5)$$

3 Results and Discussion

3.1 Characterization of biochar and ferromagnetic biochar (FMB)

The biochar's SEM image (Figure 1(a)) shows its surface porosity. In the image, it can be observed that the pores formed on the biochar surface are well defined and uniform. EDS analysis indicates higher carbon (40.01%) and oxygen (39.60%) content in biochar (Figure 1(b)). However, the elemental composition showed the presence of inorganic elements such as Cl (0.42%), Ca (1.89%), Si (0.34%) and K (17.66%).

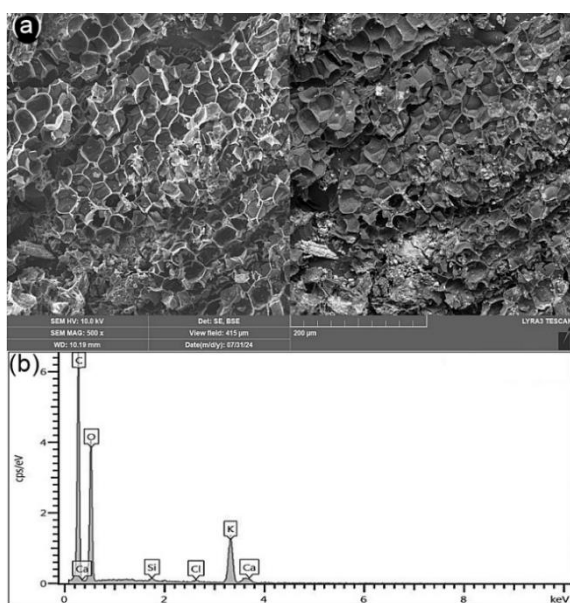


Figure 1: (a) SEM image of biochar and (b) EDS analysis of biochar.

The SEM image of FMB (Figure 2(a)) shows a homogeneous surface, the iron particles are distinguishable and it is attributed to the presence of spheres on its surface that the non-modified biochar did not show. This highlights that the biochar impregnation with iron was achieved and FMB was obtained. Figure 2(b) shows the elemental composition of FeSO₄-treated biochar determined by EDS analysis. This analysis technique was used to understand the disposition of iron in biochar and the existence of 52.95% Fe was observed after treatment. In addition, a higher C (24%) and O (21.51%) content was observed, which is similar to that observed in biochar.

The functional groups presented on the surface of biochar and FMB were determined by FTIR spectroscopy in the wavelength range of 4000 to 400 cm⁻¹. The infrared spectra are shown in Figure 3. The spectrum of biochar shows bands centered at 3163, 1652, 1539, 1394, 1002, 867 and 700 cm⁻¹. The band at 3163 cm⁻¹ is assigned to the O-H stretching of the hydroxyl group [42], [43]. The bands at 1652 and 1539 cm⁻¹ correspond to the C=O vibration of aldehydes or ketones, related to the cellulose dissociation and hemicellulose and the aromatic C=C stretching vibration [44]. The band appearing at 1394 cm⁻¹ is assigned to the symmetric bending of C-H, the band at 1002 cm⁻¹ is associated with the C-O stretching, and bands at 867 and 700 cm⁻¹ are assigned to the out-of-plane C-H bending of aromatic and the C=C bond [45], [46]. In the FTIR spectrum of the FMB, the absence of bands corresponding to symmetric C-H bending (1394 cm⁻¹), C-O stretching and C=C out-of-plane bending (700 cm⁻¹) was observed. However, new bands were observed after Fe modification biochar to obtain FMB, these bands appear at 1138, 601 and 507 cm⁻¹ and are assigned to the asymmetric stretching and bending of SO₄²⁻ and the stretching of Fe-O [47].

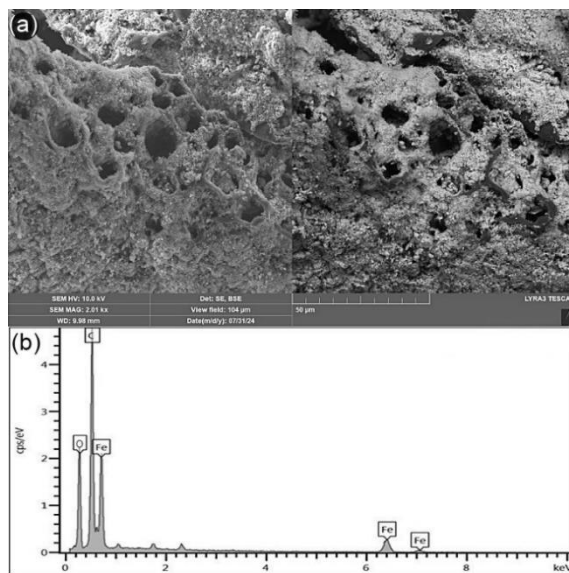


Figure 2: (a) SEM image of FMB and (b) EDS analysis of FMB.

Raman spectra of biochar and FMB are shown in Figure 4. The spectrum of biochar shows the appearance of D (1313 cm⁻¹) and G (1575 cm⁻¹) bands, which are associated with the presence of

defects in the carbon structure and the stretching vibration of carbon atom pairs (characteristic of graphite) [48]. Additionally, a weak band is observed around 498 cm^{-1} attributed to the bending vibration of C-C bonds. The FMB spectrum shows three additional bands which were identified at 213, 276 and 616 cm^{-1} , these are assigned to Fe-O_s stretching (O_s of SO₄²⁻ bridge), Fe-O stretching (O of terminal H₂O) and asymmetric bending of SO₄²⁻, respectively [49].

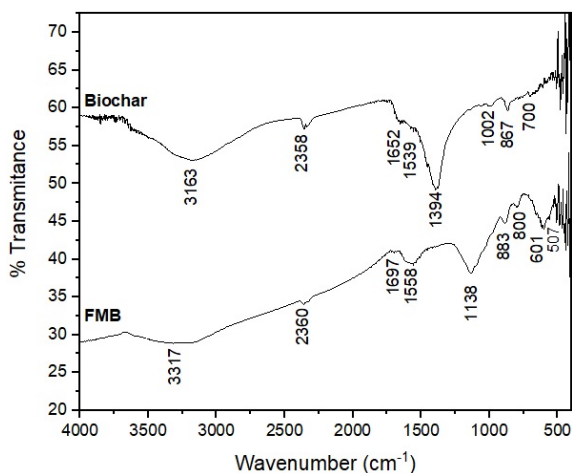


Figure 3: FTIR spectra of biochar and FMB.

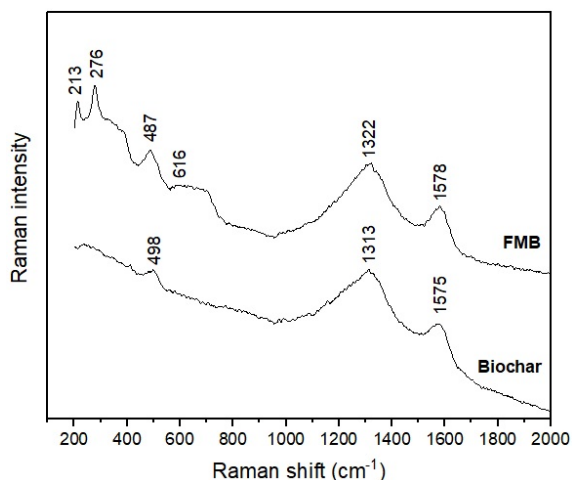


Figure 4: Raman spectra of biochar and FMB.

3.2 Dyes adsorption

FMB was used for MB and RB adsorption tests. FTIR and Raman analyses were performed on FMB after

dye adsorption tests were completed. The FTIR spectra are shown in Figure 5.

The spectrum obtained from MB adsorption (Figure 5(a)), shows three new bands which appear at 1194, 698 and 630 cm^{-1} and are assigned to the in-plane bending of the C-C heterocyclic, symmetric stretching and bending of the C-S-C [50]. In the spectrum obtained after RB adsorption (Figure 5(b)), no difference was observed with respect to the spectrum of FMB; however, a slight increase in intensity was observed in the band located between 1650 and 1470 cm^{-1} , with a maximum around 1585 cm^{-1} . This band is associated with the stretching vibration of C=N bond in the aromatic structure of RB [51].

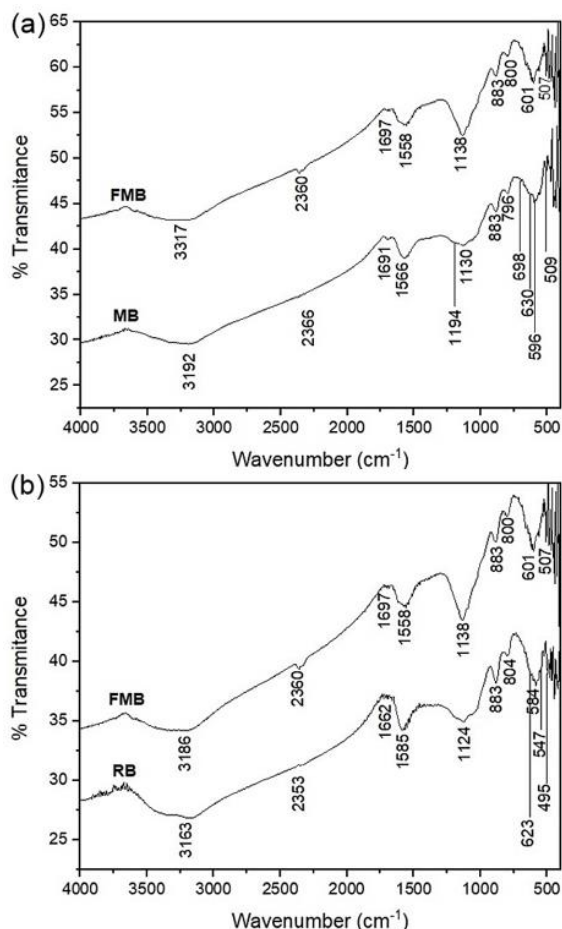


Figure 5: FTIR spectra of FMB adsorption of (a) MB and (b) RB.

The Raman spectrum of MB adsorption (Figure 6(a)), the appearance of new bands can be observed,

including two bands at 339 and 372 cm^{-1} generated by the stretching vibration of the Fe-O bond [49]. Two bands at 450 and 604 cm^{-1} were assigned to the skeletal deformation of C-N-C and C-S-C bonds, and a band at 1285 cm^{-1} corresponding to the in-plane deformation of C-H bond in the ring [52], [53]. The spectrum after adsorption of RB (Figure 6 (b)) showed two new bands centered at 388 and 593 cm^{-1} , which were assigned to torsion of xanthene ring and in-plane bending or deformation of xanthene ring, respectively [54].

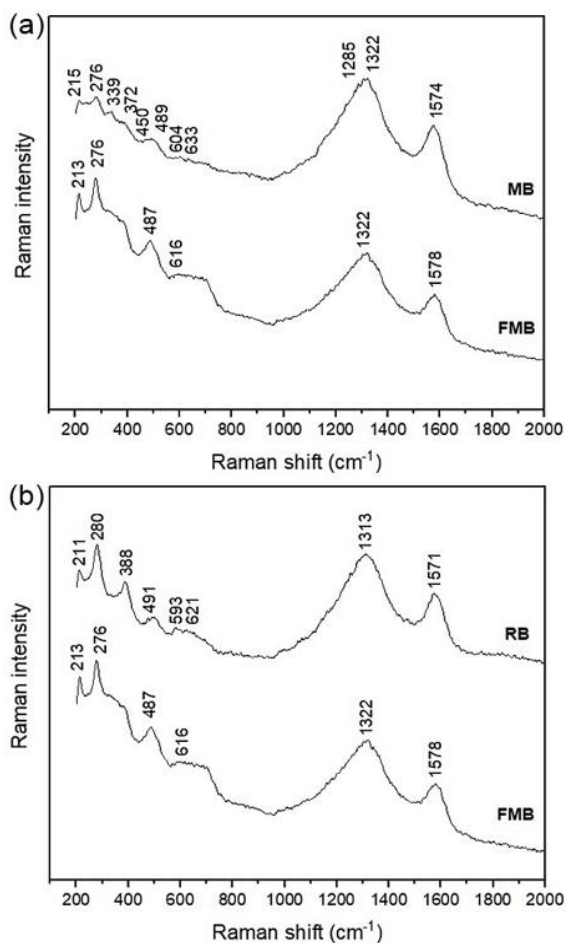


Figure 6: Raman spectra of FMB adsorption of (a) MB and (b) RB.

The change in the percentage of removal of dyes by FBC with contact time (t) is shown in Figure 7. The adsorption time of MB was 75 min and that of RB was 150 min, which remains constant after their respective times. During the experiment, 99.44% of methylene blue and 98.20% of rhodamine B were successfully

adsorbed. This means that the equilibrium time for MB and RB removal dyes by FMB is considered to be 75 min and 120 min, respectively. During the first 15 min the MB adsorption was rapid; subsequently, the adsorption rate decreased slowly and steadily until equilibrium at 75 min. On the other hand, the RB adsorption test was slow compared to the MB adsorption; however, during the first 15 min the RB adsorption was close to 50% as shown in the graph. Then, the adsorption rate slowly and steadily decreased until equilibrium at 150 min. The smaller kinetic diameter of the methylene blue molecule compared to that of rhodamine B could facilitate its incorporation into the active sites of ferromagnetic biochar, similar results were reported by Wolski *et al.*, [55]. Kumar *et al.*, [56] synthesized banana stem biochar under similar pyrolysis conditions to those in this study and achieved a maximum removal efficiency of 93.3% for methylene blue within 80 min. Similarly, Alharbi *et al.*, [57] reported using magnetic biochar derived from *Peganum harmala* with $\text{Mn-ZnFe}_2\text{O}_4$ surface treatment for water decontamination, achieving 95% rhodamine B removal within 120 min. These findings confirm that biochar derived from plant biomass has significant potential for MB and RB dye adsorption.

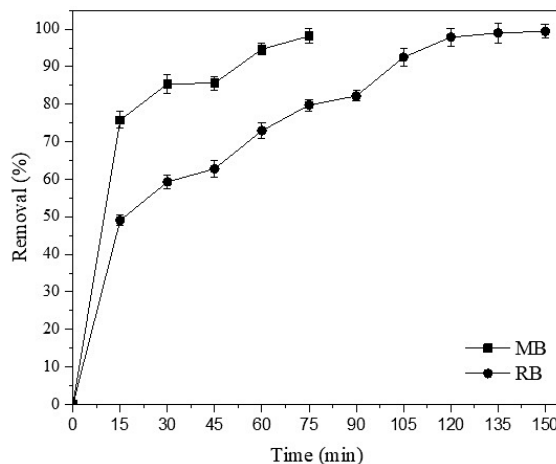


Figure 7: Effect of contact time on the elimination of MB and RB by FBC.

The adsorption kinetics process was used to examine the adsorption rate and mechanism, the pseudo-first-order model (PFO) and pseudo-second-order model (PSO) were conducted, respectively. The results are summarized in Table 1. The experimental data analyzed using the pseudo-first-order model where $\ln(q_e - q_t)$ vs. t was graphed (Figure 8(a)), it

could be interpreted that the pseudo-first-order equation does not fit the experimental analysis for MB ($R^2 = 0.7642$) and RB ($R^2 = 0.8124$) dyes. However, t/q_t vs. t was plotted (Figure 8(b)) for pseudo-second-order kinetic analysis; the R^2 values for both MB ($R^2 = 0.9911$) and RB ($R^2 = 0.9770$) dyes indicate that the second-order model is adequate to describe the adsorption kinetics. Likewise, it can be observed in Table 1 that for the adsorption experiments studied, the calculated q_e values are close to the experimental q_e values.

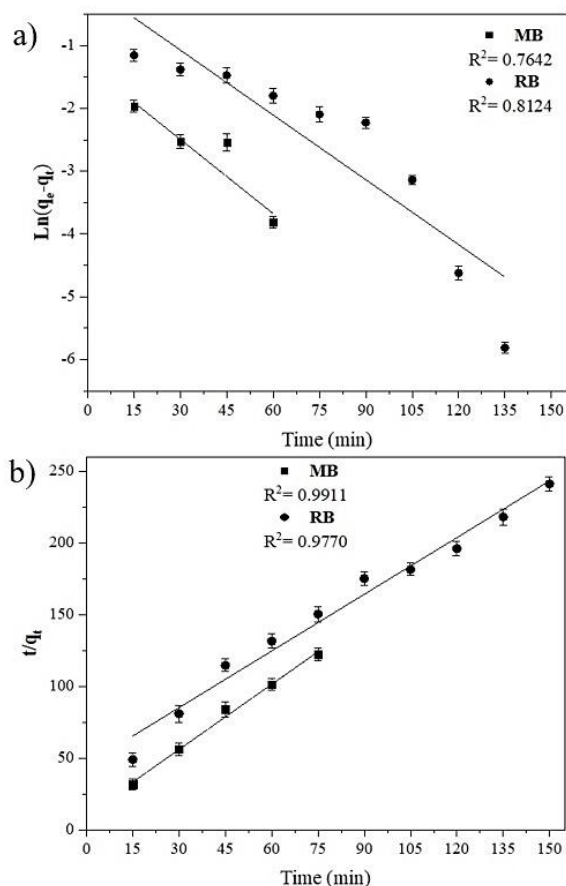


Figure 8: Linear graphs of pseudo-first-order kinetics (a) and pseudo-second-order kinetics (b) for MB and RB adsorption.

The linear graphs of the intraparticle diffusion model (IPD) are shown in Figure 9 and its parameters are presented in Table 1. IPD was used to explain the dye adsorption process on biochar. The graph of q_t vs $t^{0.5}$ of IDP should provide a straight line [58]. When the straight line crosses the origin, it means that the rate-limiting step is an intraparticle diffusion;

otherwise, the adsorption process is controlled by another mechanism. In this case, as seen in the graph (Figure 9) the graph's intersections for both MB and RB are not zero so the interparticle diffusion mechanism is not the rate-limiting step.

Table 1: Kinetic parameters model for removal of MB and RB.

Kinetic Model	Parameter	MB	RB
Pseudo-first order	q_{exp} (mg/g)	0.6136	0.6215
	q_e (mg/g)	0.2666	1.0424
	K_1 (1/min)	-0.00049	-0.00024
	R^2	0.7642	0.8124
Pseudo-second order	q_e (mg/g)	0.6627	0.7556
	K_2 (g/mg.min)	0.2029	0.0391
Intra-particle diffusion	C	0.0876	0.0637
	K (g/mg.min)	0.0684	0.0490
	R^2	0.8761	0.9672

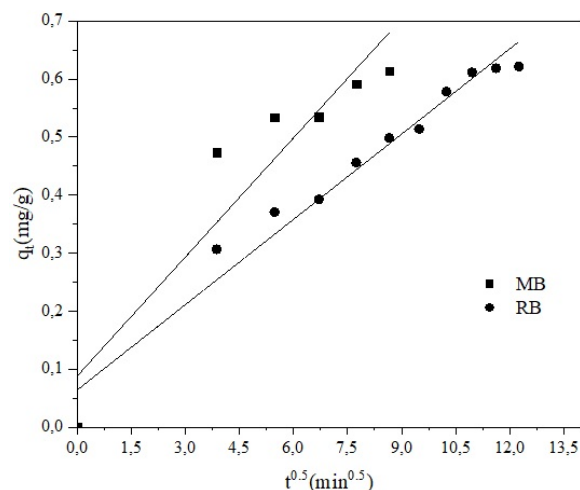


Figure 9: Linear plots of intraparticle diffusion model for MB and RB removal.

4 Conclusions

This research demonstrates the adsorption effectiveness of methylene blue and rhodamine b dyes from synthetically prepared wastewater by means of ferromagnetic biocarbon, synthesized from agricultural residues of *Musa acuminata*. The physical and chemical characterization carried out on modified biochar showed a good dispersion of Fe particles on the biochar surface, giving it ferromagnetic properties. Ferromagnetic biochar has been shown to be an effective method of adsorbing methylene blue and rhodamine b from aqueous media contaminated with these dyes. Adsorption kinetics showed that the pseudo-second-order model fit the equilibrium data

for the adsorption process of both dyes. Dye adsorption percentages of 99.44% of methylene blue and 98.20% of rhodamine b were obtained under the conditions determined for this experiment. Furthermore, the results obtained demonstrate that water contaminated with methylene blue and rhodamine b, dyes toxic to the environment, can be effectively removed, i.e. ferromagnetic biochar can be useful and effective for the treatment of effluents contaminated with dyes.

Magnetic biochar synthesis is simple to perform and economically feasible. Additionally, separating biochar after adsorption is straightforward using magnetic methods and filtration. However, further research is needed to explore methods for reusing biochar after adsorption. Moreover, scaling up methodologies from laboratory to industrial settings is essential. Future studies will focus on investigating the adsorption of larger amounts of dye in wastewater and the adsorption of heavy metals under full-scale conditions.

Acknowledgments

The authors of this paper acknowledge all the researchers at the Interdisciplinary Institute of Sciences

Author Contributions

A.G.B.: conceptualization, methodology, investigation, data analysis, supervision, review, writing and editing; M.J.A.A.: investigation, supervision, review, writing and editing; J.C.M.: review, writing, editing; D.J.M.C.: data analysis, investigation, supervision, writing and editing.

Conflicts of Interest

The authors declare that they are no conflict of interest associated with this study.

References

- [1] G. Enaïme, A. Baçaoui, A. Yaacoubi, and M. Lübken, "Biochar for wastewater treatment-conversion technologies and applications," *Applied Sciences*, vol. 10, no. 10, p. 3492, May 2020, doi: 10.3390/app10103492.
- [2] A. E. Moharm, G. A. El-Naeem, H. M. A. Soliman, A. I. Abd-Elhamid, A. A. El-Bardan, T. S. Kassem, A. A. Nayl, and S. Bräse, "Fabrication and characterization of effective biochar biosorbent derived from agricultural waste to remove cationic dyes from wastewater," *Polymers*, vol. 14, no. 13, p. 2587, 2022, doi: 10.3390/polym14132587.
- [3] Q. Chen, Q. Zhang, Y. Yang, Q. Wang, Y. He, and N. Dong, "Synergetic effect on methylene blue adsorption to biochar with gentian violet in dyeing and printing wastewater under competitive adsorption mechanism," *Case Studies in Thermal Engineering*, vol. 26, 2021, Art. no. 101099, doi: 10.1016/j.csite.2021.101099.
- [4] Y. Zhang, P. Su, D. Weathersby, Q. Zhang, J. Zheng, R. Fan, J. Zhang, and Q. Dai, "Synthesis of γ -Fe₂O₃-ZnO-biochar nanocomposites for Rhodamine B removal," *Applied Surface Science*, vol. 501, Jan. 2020, Art. no. 144217, doi: 10.1016/j.apsusc.2019.144217.
- [5] S. Wang, Y. Ruan, L. Yi, D. Liu, J. Wang, D. Fang and Z. Zhang, "Investigation on intensified degradation of Rhodamine B and heat generation using a novel thermally assisted hydrodynamic cavitation device," *Journal of Environmental Chemical Engineering*, vol. 10, Oct. 2022, Art. no. 108544, doi: 10.1016/j.jece.2022.108544.
- [6] A. K. Pandey, R. R. Kumar, B. Kalidasan, I. A. Laghary, M. Samykan, R. Khotari, A. M. Abusorrah, K. Sharma and V. V. Tyagi, "Utilization of solar energy for wastewater treatment: Challenges and progressive research trends," *Journal of Environmental Management*, vol. 297, Jul. 2021, Art. no. 113300, doi: 10.1016/j.jenvman.2021.113300
- [7] C. Kosaiyakanon, and S. Kungsanant, "Adsorption of Reactive Dyes from Wastewater Using Cationic Surfactant-modified Coffee Husk Biochar," *Environment and Natural Resources Journal*, vol. 18, no. 1, pp. 21–32, 2020, doi: 10.32526/enrj.18.1.2020.03.
- [8] M. Lewoyehu "Comprehensive review on synthesis and application of activated carbon from agricultural residues for the remediation of venomous pollutants in wastewater," *Journal of Analytical and Applied Pyrolysis*, vol. 159, Aug. 2021, Art. no. 105279, doi: 10.1016/j.jaap.2021.105279
- [9] J. Wu, J. Yang, P. Feng, G. Huang, C. Xu, and Lin B, "High-efficiency removal of dyes from wastewater by fully recycling litchi peel biochar," *Chemosphere*, vol. 246, May. 2020, Art. no. 125734 doi: 10.1016/j.chemosphere.2019.125734.

- [10] J. Wang, and S. Wang, "Preparation, modification and environmental application of biochar: A review," *Journal of Cleaner Production*, vol. 227, pp. 1002–1022, Aug. 2019, doi: 10.1016/j.jclepro.2019.04.282.
- [11] Y. Xie, L. Wang, H. Li, L. J. Westholm, L. Carvalho, E. Thorin, Z. Yu, X. Yu and Ø. Skreiberg, "A critical review on production, modification and utilization of biochar," *Journal of Analytical and Applied Pyrolysis*, vol. 161, Jan. 2022, Art. no. 125734, doi: 10.1016/j.jaap.2021.105405.
- [12] E. Viglašová, M. Galamboš, Z. Danková, L. Krivosudský, C. L. Lengauer, R. Hood-Nowotny, G. Soja, A. Rompel, M. Matík, and J. Briančin "Production, characterization and adsorption studies of bamboo-based biochar/montmorillonite composite for nitrate removal," *Waste Management*, vol. 79, pp. 385–394, Sep. 2018, doi: 10.1016/j.wasman.2018.08.005.
- [13] C. A. Odega, O. O. Ayodele, S. O. Ogutuga, G. T. Anguruwa, A. E. Adekunle, and C. O. Fakorede, "Potential application and regeneration of bamboo biochar for wastewater treatment: A review," *Advances in Bamboo Science*, vol. 2, Feb. 2023, Art. no. 100012, doi: 10.1016/j.bamboo.2022.100012.
- [14] K. Chaturvedi, A. Singhwane, M. Dhangar, M. Mili, N. Gorhae, A. Naik, N. Prashant, A. K. Srivastava, and S. Verma, "Bamboo for producing charcoal and biochar for versatile applications," *Biomass Conversion and Biorefinery*, vol. 14, pp. 15159–15185, Feb. 2024, doi: 10.1007/s13399-022-03715-3.
- [15] X. Hu, X. Zhang, H. H. Ngo, W. Guo, H. Wen, C. Li, Y. Zhang, C. Ma, "Comparison study on the ammonium adsorption of the biochars derived from different kinds of fruit peel," *Science of The Total Environment*, vol. 707, Mar. 2020, Art. no. 135544, doi: 10.1016/j.scitotenv.2019.135544.
- [16] A. Flammini, E. Brundin, R. Grill, and H. Zellweger, "Supply Chain Uncertainties of Small-Scale Coffee Husk-Biochar Production for Activated Carbon in Vietnam," *Sustainability*, vol. 12, no. 19, p. 8069, Sep. 2020, doi: 10.3390/su12198069
- [17] Y. Cao, G. Shen, Y. Zhang, C. Gao, Y. Li, P. Zhang, W. Xiao, and L. Han, "Impacts of carbonization temperature on the Pb(II) adsorption by wheat straw-derived biochar and related mechanism," *Science of The Total Environment*, vol. 692, pp. 479–489, Nov. 2019, doi: 10.1016/j.scitotenv.2019.07.102.
- [18] T. Ai, X. Jiang, Q. Liu, L. Lv, and H. Wu, "Daptomycin adsorption on magnetic ultra-fine wood-based biochars from water: Kinetics, isotherms, and mechanism studies," *Bioresource Technology*, vol. 273, pp. 8–15, Feb. 2019, doi: 10.1016/j.biortech.2018.10.039.
- [19] X. Li, Y. Cao, J. Xia, M. M. Abdus Salam and G. Chen, "Bamboo biochar greater enhanced Cd/Zn accumulation in *Salix psammophila* under non-flooded soil compared with flooded," *Biochar*, vol. 4, no. 7, Feb. 2022, doi: 10.1007/s42773-022-00139-0.
- [20] J. Su, Z. Guo, M. Zhang, Y. Xie, R. Shi, X. Huang, Y. Tuo, X. He and P. Xiang, "Mn-modified bamboo biochar improves soil quality and immobilizes heavy metals in contaminated soils," *Environmental Technology & Innovation*, vol. 34, Apr. 2024, Art. no 103630, doi: 10.1016/j.eti.2024.103630.
- [21] A. Emamverdian, A. Ghorbani, N. Pehlivan, Y. Li, M. Zargar and G. Liu, "Bamboo biochar helps minimize *Brassica* phytotoxicity driven by toxic metals in naturally polluted soils of four mine zones," *Environmental Technology & Innovation*, vol. 36, Jul. 2024, Art. no. 103753, doi: 10.1016/j.eti.2024.103753.
- [22] Z. T. Hu, Y. Ding, Y. Shao, L. Cai, Z. Y. Jin, Z. Liu, J. Zhao, F. Li, Z. Pan, X. Li and J. Zhao, "Banana peel biochar with nanoflake-assembled structure for cross contamination treatment in water: Interaction behaviors between lead and tetracycline," *Chemical Engineering Journal*, vol. 420, Apr. 2021, Art. no. 129807, doi: 10.1016/j.cej.2021.129807.
- [23] M. A. El-Nemra, M. Yilmaz, S. Ragab and A. El-Nemr, "Watermelon peels biochar-S for adsorption of Cu²⁺ from water," *Desalination and Water Treatment*, vol. 261, pp. 195–213, Jun. 2022, doi: 10.5004/dwt.2022.28506.
- [24] R. Foroutan, S. J. Peighambaroust, S. Ghojavand, S. Farjadfard and B. Ramavandi, "Cadmium elimination from wastewater using potato peel biochar modified by ZIF-8 and magnetic nanoparticle," *Colloid and Interface Science Communications*, vol. 55, May. 2023, Art. no. 100723, doi: 10.1016/j.colcom.2023.100723.
- [25] Y. Zhaoa, X. Heb, K. Qib, A. Zadac and Jing Pan, "Study on the adsorption of phosphate over biochar-based adsorbents from peanut shell and

- orange peel in water,” *Desalination and Water Treatment*, vol. 308, pp. 102–109, Oct. 2023, doi: 10.5004/dwt.2023.29810.
- [26] Y. Zhou, J. Wang, M. Sun, W. Li and X. Hu, “Adsorption of CO₂ by nitrogen doped corn straw based biochar,” *Arabian Journal of Geosciences*, vol. 14, Aug. 2021, Art. no. 1875, doi: 10.1007/s12517-021-08224-7.
- [27] C. K. C. Cabriga, K. V. B. Clarete, J. A. T. Zhang, R. M. P. Pacia, Y. S. Ko and J. C. Castro, “Evaluation of biochar derived from the slow pyrolysis of rice straw as a potential adsorbent for carbon dioxide,” *Biomass Conversion and Biorefinery*, vol. 13, pp. 7887–7894, Jun. 2021, doi: 10.1007/s13399-021-01719-z.
- [28] A. Peter, B. Chabot and E. Loranger, “Enhanced activation of ultrasonic pre-treated softwood biochar for efficient heavy metal removal from water,” *Journal of Environmental Management*, vol. 290, Apr. 2021, Art. no. 112569, doi: 10.1016/j.jenvman.2021.112569.
- [29] S. Chandra, I. Medha, J. Bhattacharya, K. R. Vanapalli and B. Samal, “Effect of the Co-Application of Eucalyptus Wood Biochar and Chemical Fertilizer for the Remediation of Multimetal (Cr, Zn, Ni, and Co) Contaminated Soil,” *Sustainability*, vol. 14, no. 12, p. 7266, Apr. 2022, doi: 10.3390/su14127266.
- [30] Y. Sun, B. Dong, L. Wang, H. Li and E. Thorin, “Technology selection for capturing CO₂ from wood pyrolysis,” *Energy Conversion and Management*, vol. 266, May. 2022, Art. no. 115835, doi: /10.1016/j.enconman.2022.115835.
- [31] S. E. Guapacha, M. Salazar, J. Aguillón, and P. Landázuri, “Similitud cariotípica entre diversas variedades de Musa spp del Quindío-Colombia,” *Cultivos Tropicales*, vol. 38, no. 4, pp. 119-126, Oct. 2017.
- [32] I. Cabeza, M. Thomas, A. Vasquez, P. Acevedo, and M. Hernandez, “Anaerobic Co-digestion of Organic Residues from Different Productive Sectors in Colombia: Biomethanation Potential Assessment,” *Chemical Engineering Transactions*, vol. 49, pp. 385–390, May. 2016, doi: 10.3303/CET1649065.
- [33] M. T. Amin, A. A. Alazba, and M. Shafiq, “Comparative study for adsorption of methylene blue dye on biochar derived from orange peel and banana biomass in aqueous solutions,” *Environmental Monitoring and Assessment*, vol. 191, Nov. 2019, Art. no. 735, doi: 10.1007/s10661-019-7915-0.
- [34] R. T. Kapoor, M. Rafatullah, M. R. Siddiqui, M. A. Khan, and M. Sillanpää “Removal of reactive black 5 dye by banana peel biochar and evaluation of its phytotoxicity on tomato,” *Sustainability*, vol. 14, no. 7, p. 4176, Mar. 2022, doi: 10.3390/su14074176.
- [35] S. Daffalla, A. Taha, E. Da’na and M. R. El-Aassar, “Sustainable banana-waste-derived biosorbent for congo red removal from aqueous solutions: Kinetics, equilibrium, and breakthrough studies,” *Water*, vol. 16, no. 10, p. 1449, May. 2024, doi: 10.3390/w16101449.
- [36] F. Fuentes-Gandara, I. Piñeres-Ariza, A. Zambrano-Arevalo, G. Castellar-Ortega, C. Herrera-Herrera, S. Castro-Muñoz, G. Peluffo-Foliaco and J. Pinedo-Hernández, “Removal of direct navy blue dye from aqueous solutions using banana peels,” *Global Journal of Environmental Science and Management*, vol. 10, no. 3, pp. 1067–1084, Apr. 2024, doi: 10.22034/gjesm.2024.03.09.
- [37] B. Sajjadi, R. M. Shrestha, W. Y. Chen, D. L. Mattern, N. Hammer, V. Raman and A. Dorris, “Double-layer magnetized/functionalized biochar composite: Role of microporous structure for heavy metal removals,” *Journal of Water Process Engineering*, vol. 39, Feb. 2021, Art. no. 101677, doi: 10.1016/j.jwpe.2020.101677.
- [38] M. D. Gillingham, R. L. Gomes, R. Ferrari and H. M. West, “Sorptions, separation and recycling of ammonium in agricultural soils: A viable application for magnetic biochar?,” *Science of the Total Environment*, vol. 812, Mar. 2022, Art. no. 151440, doi: 10.1016/j.scitotenv.2021.151440.
- [39] A. Tomczyk, Z. Sokołowska and P. Boguta, “Biochar physicochemical properties: Pyrolysis temperature and feedstock kind effects,” *Reviews in Environmental Science and Bio/Technology*, vol. 19, pp. 191–215, Feb. 2020, doi: 10.1007/s11157-020-09523-3.
- [40] A. Bopda, S. G. Mokue Mafo, J. N. Ndongmo, G. T. Kenda, C. G. Fotsop, I. H. Tiotsop Kuete, C. S. Ngakou, D. R. Tchoufon Tchoufon, A. Tamo A, G. N. A. Nche, and S. G. Anagho SG, “Ferromagnetic biochar prepared from hydrothermally modified calcined mango seeds for fenton-like degradation of indigo carmine,” *C*, vol. 8, no. 4, p. 81, Dec. 2022, doi: 10.3390/c8040081.
- [41] R. Isaac and S. Siddiqui, “Sequestration of Ni(II) and Cu(II) using FeSO₄ modified Zea mays husk magnetic biochar: Isotherm, kinetics,

- thermodynamic studies and RSM,” *Journal of Hazardous Materials Advances*, vol. 8, Sep. 2022, Art. no. 100162, doi: 10.1016/j.hazadv.2022.100162.
- [42] A. Y. Elnour, A. A. Alghyamah, H. M. Shaikh, A. M. Poulouse, S. M. Al-Zahrani, A. Anis, and M. I. Al-Wabel, “Effect of pyrolysis temperature on biochar microstructural evolution, physicochemical characteristics, and its influence on biochar/polypropylene composites,” *Applied Sciences*, vol. 9, no. 6, p. 1149, Mar. 2019, doi: 10.3390/app9061149.
- [43] R. Janu, V. Mrlik, D. Ribitsch, J. Hofman, P. Sedláček, L. Bielská, and G. Soja, “Biochar surface functional groups as affected by biomass feedstock, biochar composition and pyrolysis temperature,” *Carbon Resources Conversion*, vol. 4, p.p. 36–46, 2021, doi: 10.1016/j.crcon.2021.01.003.
- [44] L. Suárez-Hernández, A.N. Ardila-A, and R. Barrera-Zapata, “Morphological and physicochemical characterization of biochar produced by gasification of selected forestry species,” *Revista Facultad de Ingeniería*, vol. 26, no. 46, pp. 123–130, Sep. 2017, doi: 10.19053/01211129.v26.n46.2017.7324.
- [45] T. Yang, J. Meng, P. Jeyakumar, T. Cao, Z. Liu, T. He, X. Cao, W. Chen, and H. Wang “Effect of pyrolysis temperature on the bioavailability of heavy metals in rice straw-derived biochar,” *Environmental Science and Pollution Research*, vol. 28, no. 2, pp. 2198–2208, Sep. 2020, doi: 10.1007/s11356-020-10193-5.
- [46] M. Wu, Q. Feng, X. Sun, H. Wang, G. Gielen, and W. Wu, “Rice (*Oryza sativa* L) plantation affects the stability of biochar in paddy soil,” *Scientific Reports*, vol. 5, May 2015, Art. no. 10001, doi: 10.1038/srep10001.
- [47] V. Rouchon, H. Badet, O. Belhadj, O. Bonnerot, B. Lavédrine, J. G. Michard, and S. Miska, “Raman and FTIR spectroscopy applied to the conservation report of paleontological collections: identification of Raman and FTIR signatures of several iron sulfate species such as ferrinatriite and sideronatriite,” *Journal of Raman Spectroscopy*, vol. 43, pp. 1265–1274, Jun. 2012, doi: 10.1002/jrs.4041.
- [48] T. A. Saleh, and A. A. Al-Saadi, “Surface characterization and sorption efficacy of tire-obtained carbon: experimental and semiempirical study of rhodamine B adsorption,” *Surface and Interface Analysis*, vol. 47, pp. 785–792, May. 2015, doi: 10.1002/sia.5775.
- [49] C. H. Chio, S. K. Sharma, and D. W. Muenow, “The hydrates and deuterates of ferrous sulfate (FeSO₄): a Raman spectroscopic study,” *Journal of Raman Spectroscopy*, vol. 38, pp. 87–99, Sep. 2007, doi: 10.1002/jrs.1623.
- [50] O. V. Ovchinnikov, A. V. Evtukhova, T. S. Kondratenko, M. S. Smirnov, Y. V. Khokhlov, and O. V. Erina, “Manifestation of intermolecular interactions in FTIR spectra of methylene blue molecules,” *Vibrational Spectroscopy*, vol. 86, pp. 181–189, Sep. 2016, doi: 10.1016/j.vibspec.2016.06.016.
- [51] W. Rao, P. Piliouras, X. Wang, A. Guido, K. Kugler, B. Sieren, L. Wang, G. Lv, Z. Li, “Zwitterionic dye rhodamine B (RhB) uptake on different types of clay minerals,” *Applied Clay Science*, vol. 197, Nov. 2020, Art. no. 105790, doi: 10.1016/j.clay.2020.105790.
- [52] C. Li, Y. Huang, K. Lai, B. A. Rasco, and Y. Fan “Analysis of trace methylene blue in fish muscles using ultra-sensitive surface-enhanced Raman spectroscopy,” *Food Control*, vol. 65, pp. 99–105, Jul. 2016, doi: 10.1016/j.foodcont.2016.01.017.
- [53] K. T. Tu, and C. K. Chung, “Enhancement of Surface Raman Spectroscopy Performance by Silver Nanoparticles on Resin Nanorods Arrays from Anodic Aluminum Oxide Template,” *Journal of The Electrochemical Society*, vol. 164, no. 5, pp. B3081–B3086, Jan. 2017, doi: 10.1149/2.0121705jes.
- [54] S. Lin, W. L. J. Hasi, X. Lin, S. Han, X. T. Lou, F. Yang, D. Y. Lin, and Z. W. Lu, “Rapid and sensitive SERS method for determination of Rhodamine B in chili powder with paper-based substrates,” *Analytical Methods*, vol. 7, pp. 5289–5294, May 2015, doi: 10.1039/C5AY00028A.
- [55] R. Wolski, A. Bazan-Wozniak, A. Nosal-Wiercinska and R. Pietrzak, “Methylene blue and rhodamine B dyes’ efficient removal using biocarbons developed from waste,” *Molecules*, vol. 29, no. 17, p. 4022, Aug. 2024, doi: 10.3390/molecules29174022.
- [56] U. Kumar, B. Vibhute, N. Sharma and A. Sahay, “Efficient removal of methylene blue dye by alkaline-treated banana stem biochar through adsorption method,” *Applied Ecology and Environmental Sciences*, vol. 10, no. 4, pp. 236–243, Apr. 2022, doi: 10.12691/aees-10-4-8.
- [57] A. F. Alharbi, A. A. Alotaibi, H. E. M. Gomaa, A. A. M. Abahussain, and S. M. A. Azeem,



“Magnetic biochar by one-step impregnation pyrolysis of *Peganum harmala L.* for removal of rhodamine B,” *Adsorption Science & Technology*, vol. 2023, Aug. 2023, doi: 10.1155/2023/9993465.

[58] S. Nirmaladevi, and N. Palanisamy, “A comparative study of the removal of cationic and anionic dyes from aqueous solutions using biochar as an adsorbent,” *Desalination and Water Treatment*, vol. 175, pp. 282–292, Jan. 2020, doi: 10.5004/dwt.2020.24906.